Research Article

Francesco Baino* and Elisa Fiume

Modelling the elastic mechanical properties of bioactive glass-derived scaffolds

https://doi.org/10.1515/bglass-2020-0005
Received Sep 01, 2020; revised Oct 14, 2020; accepted Nov 21, 2020

Abstract: Porosity is known to play a pivotal role in dictating the functional properties of biomedical scaffolds, with special reference to mechanical performance. While compressive strength is relatively easy to be experimentally assessed even for brittle ceramic and glass foams, elastic properties are much more difficult to be reliably estimated. Therefore, describing and, hence, predicting the relationship between porosity and elastic properties based only on the constitutive parameters of the solid material is still a challenge. In this work, we quantitatively compare the predictive capability of a set of different models in describing, over a wide range of porosity, the elastic modulus (7 models), shear modulus (3 models) and Poisson's ratio (7 models) of bioactive silicate glass-derived scaffolds produced by foam replication. For these types of biomedical materials, the porosity dependence of elastic and shear moduli follows a second-order power-law approximation, whereas the relationship between porosity and Poisson's ratio is well fitted by a linear equation.

Keywords: scaffold; bioglass; mechanical properties

1 Introduction

When tissue regeneration is a goal, implantable biomaterials are often designed as porous scaffolds that serve as three-dimensional (3D) templates to support and guide the healing of healthy tissue at the injured site [1]. In bone tissue engineering strategies, bioactive man-made materials are highly attractive as they allow overcoming the various limitations of transplant procedures, including the need for extra-surgery/shortage of transplant material if autografts are used and the risk of disease transmission as well as ethical/religious concerns in the case of allografts and xenografts [2].

Bioactive glasses are excellent candidates for scaffolding in osseous repair due to their ability of bonding to host bone [3–5] and stimulating osteogenesis via the release of therapeutically-active ionic dissolution products (*e.g.* Ca^{2+} and silicate ions) that elicit cell responses towards a path of regeneration and self-repair [6–8].

Scaffolds for bone substitution should fulfill a set of physico-chemical and biological properties, including biocompatibility and similarity to natural bone in terms of pore-strut architecture and mechanical characteristics [9]. Assuming that an ideal scaffold should mimic the structure of human cancellous bone, a total porosity of 50 vol.% (minimum) and a pore size above 100 μm are typically recommended to allow adequate perfusion of biological fluids and nutrients, cell colonization, and vascularization [10]. Microstructure and porosity also dictate the mechanical properties of the scaffold, such as strength and elastic modulus. While the compressive strength of bioactive glass scaffolds is relatively easy to assess and, then, to correlate with porosity, the Young's modulus and other elastic properties are much more difficult to determine without a proper equipment; in general, this is a common problem for brittle, highly-porous ceramics. The knowledge of the elastic modulus, however, is key to determine the biomechanical success of an implantable biomaterial as a good stiffness match between scaffold and host tissue allows favorable stress transfer, thereby yielding stable interfacial bonding and osteointegration [11].

Therefore, quantifying the relationship between the internal structure and elastic mechanical properties of biomaterials still remain a partially unmet challenge. Some attempts have been published in the literature but most of them are based on the interpolation of experimental data by linear or polynomial functions in specific cases rather than on general physical models. Sanz-Herrera *et al.* [12] reported that a second-order polynomial function (correlation coefficient R^2 = 0.998) can describe the Young's

***Corresponding Author: Francesco Baino:** Institute of Materials Physics and Engineering, Department of Applied Science and Technology, Politecnico di Torino, Corso Duca degli Abruzzi 24, 10129 Torino, Italy; Email: francesco.baino@polito.it; Tel.: +39 011 090 4668; Fax: +39 011 090 4624
Elisa Fiume: Institute of Materials Physics and Engineering, Department of Applied Science and Technology, Politecnico di Torino, Corso Duca degli Abruzzi 24, 10129 Torino, Italy

modulus of scaffolds with face-centered cubic (FCC) structure over the entire range of investigated porosities (1.2-89.6 vol.%), while a highly linear negative relationship (R^2 = 0.999) exists if the pore range is restricted to 30-80 vol.%. In another study, after elaborating experimental data obtained from ultrasonic wave propagation measurements [13], Gerhardt and Boccaccini [14] found a linear negative correlation (R^2 = 0.866) between porosity and elastic modulus of 45S5 Bioglass® foams.

Indeed, the ideal, highly-ambitious aim would be to develop and apply a theory that employs general microstructural information (*e.g.* the constitutive properties of solid skeleton) to make accurate predictions. In this regard, Fu *et al.* [15] applied the density power-law model (Gibson's model) to estimate the elastic modulus (3 GPa) of 13-93 bioactive glass scaffolds (total porosity 85 vol.%) produced by sponge replication. Baino and Fiume [16] applied the same model to predict the Young's modulus of 45S5 Bioglass® foams and proved its good predictive capability (R^2 = 0.8953) over a wide range of porosities (52-86 vol.%).

In order to further expand the knowledge in this field, the present work aims at comparing the suitability of a set of physico-mathematical models (17 equations) in describing the relationship between porosity and elastic properties (*i.e.* elastic modulus, shear modulus, and Poisson's ratio) of glass-derived foam-like scaffolds. To the best of the authors' knowledge, it is the first time that such a broad comparative study is performed on biomedical scaffolds.

2 Materials and methods

2.1 Scaffolds

The models described in the section 2.2 were applied to two sets of bioactive silicate glass-derived scaffolds, the elastic properties of which were experimentally determined in a couple of previous works [16, 17]. Both sets of samples were fabricated by sponge replica method, which is very suitable to obtain bone-like structures with open and interconnected macropores [18]. The first set of data comprised the elastic modulus, shear modulus and Poisson's ratio of 45S5 Bioglass®-based glass-ceramic scaffolds (basic oxide system: $45SiO_2$–$24.5CaO$–$24.5Na_2O$–$6P_2O_5$ wt.%) with porosity within 52-86 vol.%; these mechanical properties were non-destructively assessed by the impulse excitation technique (GrindoSonic system) [16]. The second set of data comprised the elastic modulus of CEL2-based glass-ceramic scaffolds (basic oxide system: $43.8SiO_2$–$23.6CaO$–$4.6MgO$–$15.0Na_2O$–$6.1K_2O$–$6.9P_2O_5$ wt.%) with porosity within 42-77 vol.%; this mechanical property was assessed by ultrasonic testing [17]. The experimental characterization of these scaffolds was reported in those previous studies.

2.2 Modelling

The macroscopic elastic properties of 3D isotropic porous materials, such as foam-like scaffolds, can be characterized by two independent parameters, *i.e.* Young's modulus (E) and Poisson's ratio (ν). The shear modulus (G) is often calculated on the basis of E and ν through appropriate models or computations.

The assumption of isotropic porous solid for foam-replicated scaffolds is made on the basis of previous investigations. Falvo D'Urso Labate *et al.* [19] reported that the degree of anisotropy (DA) of CEL2-derived scaffolds produced by sponge replication was below 0.15. DA provides a measure of the preferential alignment of solid struts in a scaffold along particular directions. In that study, DA was estimated by the mean intercept length (MIL) analysis applied to micro-computed tomographic reconstructions. DA can range from 0 (overall scaffold isotropy) and 1 (overall scaffold anisotropy) and, therefore, the assumption of isotropic scaffolds closely approaches reality.

In general, we expect the elastic properties of porous scaffolds to depend on both the constitutive properties of the solid matrix (E_0, G_0, ν_0) and the relative density (φ). The total porosity can be expressed as ($1 - \varphi$), and the form of the functions relating E, G and ν to E_0, G_0, ν_0 and φ depends on microstructure. Hence, any meaningful models describing these relationships should be developed by considering the salient structural characteristics of scaffolds. Therefore, in this work the early selection of models was performed on the basis of their relevance in describing foam-like structures (*i.e.* similar to 45S5 and CEL2 glass-derived scaffolds).

Perhaps the most common and easy-to-apply models used to estimate E and G of porous solids are those developed by Gibson and Ashby in 1982 [20]. They demonstrated that the elastic and shear moduli of low-density open-cell ceramics (foams) are primarily dictated by the relative density according to a power law (second order), as follows:

$$E = E_0 \varphi^2 \tag{1}$$

$$G = \frac{3}{4} G_0 (1 + \nu_0) \varphi^2 \tag{2}$$

Determination of the Poisson's ratio ν is, in general, much more difficult; especially for highly-porous materials, its assessment has been a challenge from both theoretical and experimental viewpoints. Arnold *et al.* [21] developed a general equation for the prediction of the Poisson's ratio of porous materials, which was strictly derived for spherical porosity and isotropic materials (like the glass scaffolds investigated in this work) and was valid over the whole porosity range:

$$\nu = 0.5 - \frac{3}{4}\varphi(1 - \nu_0) \tag{3}$$

Warren and Kraynik [22] developed a 3D foam model using the tetrahedral unit cell to investigate the macroscopic properties of open-cell foams; specifically, the elastic parameters E and ν were calculated as:

$$E = \frac{E_0\varphi^2\,(11 + 4\varphi)}{10 + 31\varphi + 4\varphi^2} \tag{4}$$

$$\nu = \frac{(1 - \varphi)\,(5 + 4\varphi)}{10 + 31\varphi + 4\varphi^2} \tag{5}$$

Zhu *et al.* [23] adopted a tetrakaidekahedral cell-based lattice to model open-cell foams:

$$E = \frac{0.726E_0\varphi^2}{1 + 1.09\varphi} \tag{6}$$

$$\nu = 0.5\left(\frac{1 - 1.09\varphi}{1 + 1.09\varphi}\right) \tag{7}$$

$$G = \frac{0.2333E_0\varphi^2}{1 + 0.700\varphi} \tag{8}$$

The same authors also proposed a variation of these equations under the assumption, first introduced by Kraynik and Warren [24], that the edge cross-sections are plateau borders rather than equilateral triangles:

$$E = \frac{1.009E_0\varphi^2}{1 + 1.514\varphi} \tag{9}$$

$$\nu = 0.5\frac{1 - 1.514\varphi}{1 + 1.514\varphi} \tag{10}$$

$$G = \frac{0.32E_0\varphi^2}{1 + 0.96\varphi} \tag{11}$$

While the Equations (1)–(11) are obtained from analytical calculations based on physical and geometrical models, some more recent approaches rely on a combination between theory and finite element modelling (FEM). Gan *et al.* [25] used random 3D Voronoi cells to build the whole open-cell foam; the curve fitting to the results of FEM analysis yielded the predictive equations for the elastic parameters:

$$E = \frac{E_0\varphi^2}{1 + 6\varphi} \tag{12}$$

$$\nu = \nu_0 + (0.5 - \nu_0)\frac{1 - \varphi}{1 + 14\varphi} \tag{13}$$

Highly-accurate numerical methods were also proposed by Roberts and Garboczi [26] to predict the elastic properties of a number of random porous materials, including structures with open-cell intersections that closely approximate foam-like scaffolds. In this specific case, two different equations were obtained to estimate E according to the relative density:

$$E = E_0\left(\frac{\varphi - \varphi_0}{1 - \varphi_0}\right)^m,\ \varphi > 0.20 \tag{14}$$

$$E = E_0 C\varphi^n,\ \varphi \le 0.20 \tag{15}$$

and one general equation to estimate the Poisson's ratio:

$$\nu = \nu_0 + \frac{1 - \varphi}{1 - \varphi_1}(\nu_1 - \nu_0) \tag{16}$$

The constants φ_0, m, n, C, φ_1 and ν_1 were numerically determined ($\varphi_0 = 0.029$, $m = 2.15$, $n = 3.15$, $C = 4.2$, $\varphi_1 = 0.114$ and $\nu_1 = 0.233$).

A similar approach was reported by Nie *et al.* [27] who developed random 3D Laguerre-Voronoi computational models for open cell foams; curve fitting of FEM results yielded this couple of equations:

$$E = E_0\left[3.32(1 - \varphi)^3 - 7.37(1 - \varphi)^2 + 4.98\,(1 - \varphi) - 0.92\right] \tag{17}$$

$$\nu = \nu_0\left[20.68(1 - \varphi)^3 - 42.09(1 - \varphi)^2 + 30\,(1 - \varphi) - 6.91\right] \tag{18}$$

We applied the different potentially-suitable models of Equations (1)-(18) to estimate the elastic properties of 45S5- and CEL2-based glass scaffolds and quantified their predictive capability by calculating the correlation coefficient R^2 through the least-squares method (Matlab, MathWorks, Natick, MA, USA).

3 Results and discussion

Information on the elastic properties of porous scaffolds is needed for a complete interpretation of their mechanical behavior and response in given biomedical environments and applications. Such properties, which are often difficult to determine experimentally for highly-porous ceramics and glasses, are typically dictated by total porosity that,

on the contrary, is relatively easy to assess through density measurement or imaging techniques. Therefore, the use of appropriate models relating elastic properties to relative density (φ) or, conversely, total porosity ($1 - \varphi$) can be a useful tool to predict the mechanical performance of scaffolds and optimize their design and fabrication process.

Figures 1 and 2 report the experimental data for the elastic moduli of 45S5- and CEL2-derived scaffolds, respectively, along with the models described by Equations (1), (4), (6), (9), (12), (14), (15) and (17). Although both sets of scaffolds were produced by the same fabrication methods (foam replication), some differences deserve to be highlighted. In general, all the models predict the decrease of elastic modulus with increasing porosity if $\varphi < 0.5$; this trend is mostly followed in the low-porosity range ($\varphi > 0.5$) except for the Gan's model, which shows an obvious deviation from physical reality (negative values for the elastic modulus in Figure 2). As displayed in Tables 1 and 2, both Gibson's and Roberts' models have a quite high value of R^2, which suggests the good predictive capability of such models in describing the E-φ relationship for both sample batches. In the case of Roberts' model, Equation (14) was implemented for CEL2-based scaffolds ($\varphi > 0.20$), while a double-stage function was implemented for

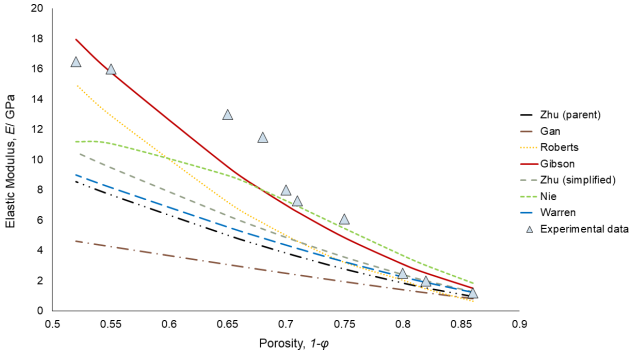

Figure 1: Porosity dependence of elastic modulus E in 45S5 glass-derived foam-like scaffolds: model comparison

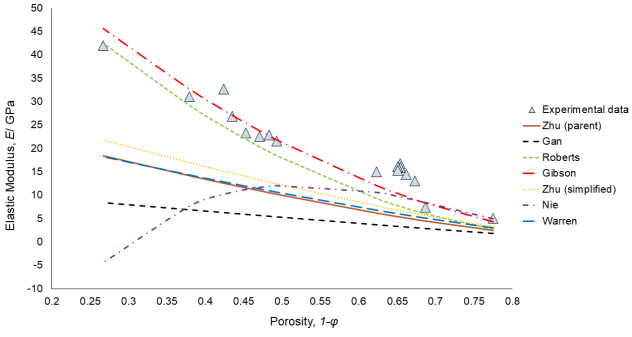

Figure 2: Porosity dependence of elastic modulus E in CEL2 glass-derived foam-like scaffolds: model comparison

Table 1: 45S5 glass-derived scaffolds: correlation coefficients for the models describing the porosity-elastic modulus relationship

Model	Equation	R^2
Gibson	(1)	0.8953
Warren	(4)	0.1359
Zhu (parent)	(6)	0
Zhu (simplified)	(9)	0.3629
Gan	(12)	0
Roberts	(14), (15)	0.6463
Nie	(17)	0.7058

Table 2: CEL2 glass-derived scaffolds: correlation coefficients for the models describing the porosity-elastic modulus relationship

Model	Equation	R^2
Gibson	(1)	0.8378
Warren	(4)	0
Zhu (parent)	(6)	0
Zhu (simplified)	(9)	0
Gan	(12)	0
Roberts	(14)	0.6303
Nie	(17)	0

45S5-derived samples, comprising Equation (14) if $\varphi > 0.20$ or Equation (15) if $\varphi < 0.20$ (highly-porous scaffolds). On the contrary, Zhu's, Warren's and Gan's models cannot be applied for both sets of data (R^2equal to zero or extremely low). The Zhu's simplified model (Equation (9)) has a moderate predictive capability only for 45S5-based scaffolds ($R^2 = 0.3629$); in this case, the estimated values of E are around 38% higher than those predicted through the "parent" model (Equation (6)) [23]. Similarly, the Nie's model also exhibits a good predictive capability only for 45S5-derived scaffolds ($R^2 = 0.7058$). Upon comparing the R^2 values, Gibson's model provides the best fitting of elastic modulus for both types of data over the whole porosity range ($R^2 > 0.83$). The Gibson's power-law model was also proved to be successful in describing the E-φ relationship of cancellous bone [28], which should be ideally mimicked by foam-like scaffolds. However, it is interesting to observe that, at high porosity, Nie's model also offers good predictions for both scaffold types (if $\varphi \leq 0.30$), with $R^2 = 0.91$ and $R^2 = 0.68$ for 45S5- and CEL2- based scaffolds, respectively, while the Zhu's simplified model provides a good data fitting only for 45S5 scaffolds ($\varphi \leq 0.20$; $R^2 = 0.99$).

The relevant model developed by Gibson and Ashby (Equation (2)) is also the most suitable one to approximate the behaviour of shear modulus, while the two models de-

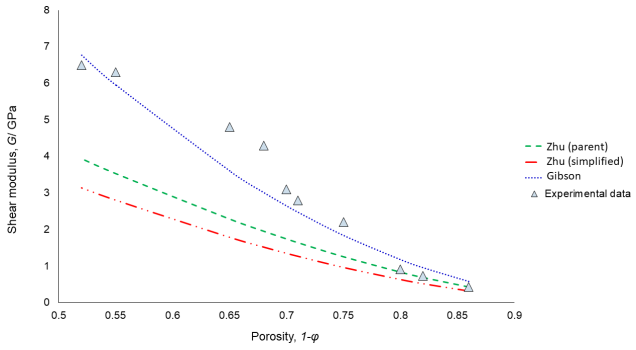

Figure 3: Porosity dependence of shear modulus G in 45S5 glass-derived foam-like scaffolds: model comparison

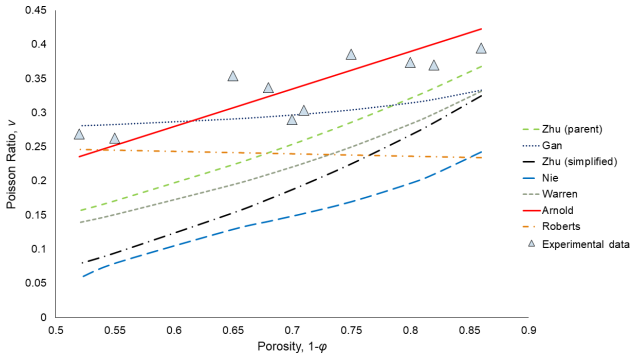

Figure 4: Porosity dependence of Poisson's ratio ν in 45S5 glass-derived foam-like scaffolds: model comparison

Table 3: 45S5 glass-derived scaffolds: correlation coefficients for the models describing the porosity-shear modulus relationship

Model	Equation	R^2
Gibson	(2)	0.9129
Zhu (parent)	(8)	0.3224
Zhu (simplified)	(11)	0

Table 4: 45S5 glass-derived scaffolds: correlation coefficients for the models describing the porosity-Poisson's ratio relationship

Model	Equation	R^2
Arnold	(3)	0.5645
Warren	(5)	0
Zhu (parent)	(7)	0
Zhu (simplified)	(10)	0
Gan	(13)	0
Roberts	(16)	0
Nie	(18)	0

veloped by Zhu *et al.* [23] (Equation (8) and (11)) exhibit poor predictive capability (Figure 3 and Table 3).

Figure 4 reports the experimental data for the Poisson's ratio of 45S5-derived scaffolds, along with the models described by Equations (3), (5), (7), (10), (13), (16) and (18). As shown in Table 4, only the Arnold's model provides an acceptable predictive capability for this set of data (R^2 = 0.5645). Most models suggest the increase of Poisson's ratio with increasing porosity, except for the Roberts' model. It is worth pointing out that the exact relationship between Poisson's ratio and porosity in porous solids is still partially unclear. While it is usually recognized that the porosity dependence of Poisson's ratio can vary according to the level of porosity considered, elucidating this relationship is difficult as the experimental measurement of Poisson's ratio is really challenging and typically requires proper equipment and samples with "*ad hoc*" geometry; hence, there is a paucity of relevant data in the literature, especially for biomedical materials. On the basis of experimental data from gel-derived silica, Arnold *et al.* [21] suggested that the Poisson's ratio increases or decreases if porosity is above or below 40 vol.%, respectively. This is consistent with the trend of experimental data reported in Figure 4 as regards the high-porosity range, and is also in line with the results reported by De With [29], who analyzed porous hydroxyapatite with porosity in the range of 3 to 27 vol.% and actually observed a decreasing trend of Poisson's ratio for increasing porosity (low-porosity range). A comprehensive study published by Yu *et al.* [30] suggested that he effective Poisson's ratio of natural ceramics (rocks) can increase, decrease or remain invariable with increasing porosity for the materials with $\nu_0 < 0.2$, $\nu_0 > 0.2$ and $\nu_0 = 0.2$, respectively. On this point, it is important to underline that porosity in natural rocks is typically low (well below 40 vol.%) and, thus, the observations reported by Yu *et al.* [30] are actually consistent with those of Arnold *et al.* [21] for low-porosity materials. Furthermore, such relationship involving ν, ν_0 and porosity is in good agreement with the conclusions reported by Roberts and Garboczi [26], whose model, however, does not approximate the trend of the experimental data from 45S5-derived scaffolds. This is probably due to the inherent limitations of the differential method that was used to develop the model, which does not give a reasonable prediction for materials with low solid fraction ($\varphi < 0.4$) [31] like biomedical scaffolds for bone repair. Hence, especially as regards the estimation of Poisson's ratio, highly-porous materials seem to represent a worst-case scenario for predictive methods; although being difficult the inclusion of high-order microstructural information [32] could be considered to improve the accuracy and predictive capability of the relevant models.

The models implemented in the present work are described by "ready-to-use" equations that can be immedi-

ately applied by researchers/users, provided that the constitutive properties of the solid matrix (E_0, G_0, ν_0) are known. In recent years, a more advanced methodology to predict the mechanical behaviour of biomedical scaffolds has been proposed by applying the theory of continuum micromechanics and homogenization. Since the mid 2000s [33], this strategy has been applied to model a range of ceramic (*e.g.* hydroxyapatite [34]) and glass-derived porous scaffolds [35, 36], yielding good predictive results provided that not only the "bulk" mechanical properties but also the micro-architectural characteristics of scaffolds are known and quantifiable. However, the modelling procedure is often quite complex and 3D volume reconstructions of scaffold architecture (*e.g.* generated by micro-computed tomographic investigation) are typically required.

Looking at the future, further improvements in the predictive capability could be achieved by applying molecular dynamics simulations and machine learning approaches, which are already implemented for the design of bioactive glasses to tailor specific properties, such as density, dissolution kinetics and bioactivity, or model the biological response, such as the glass ability to foster protein adsorption, cell adhesion, cell proliferation and antibacterial effects [37, 38]. Indeed, a critical issue to be considered concerns the incorporation of scaffold microstructure in the simulation and modelling procedures, carrying the risk to further increase the algorithmic complexity and computational cost.

4 Conclusions

The porosity dependence of elastic and shear moduli in glass-derived foams is well described ($R^2 > 0.83$) by second-order power-law models (Gibson's models) over a quite wide porosity range around 40-85 vol.%, which is the typical range of human healthy cancellous bone and, thus, is recommended for biomedical scaffolds. Roberts' and Nie's numerical models are also suitable to describe the relationship between porosity and elastic modulus, but their predictive capability is lower (R^2 within 0.60-0.70). Other models exhibit good predictive capability only at high porosity (> 70 vol.%). In general, the results reported in this study suggest that many of existing models partly fail in predicting the elastic and shear moduli of foam-like glass-derived scaffolds over the entire porosity range required for bone tissue engineering applications, but the predictions can be acceptable for highly-porous structures.

The porosity dependence of Poisson's ratio in 45S5 glass-derived foams is approximated by a negative linear correlation (Arnold's model); further theoretical and computational studies deserve to be carried out on this point to improve the predictive ability.

Ethical approval: The conducted research is not related to either human or animals use.

Conflict of Interests: The authors declare no conflict of interest regarding the publication of this paper.

References

[1] Baino F. *et al.*, Processing methods for making porous bioactive glass-based scaffolds - A state-of-the-art review, Int. J. Appl. Ceram. Technol. 2019, 16, 1762-1796.
[2] Campana V. *et al.*, Bone substitutes in orthopaedic surgery: from basic science to clinical practice, J. Mater. Sci. Mater. Med. 2014, 25, 2445-2461.
[3] Hench L.L., The story of bioglass, J. Mater. Sci. Mater. Med. 17, 967-978 (2006).
[4] Jones J., Review of bioactive glass: from Hench to hybrids, Acta Biomater. 2013, 9, 4457-4486.
[5] Fiume E., Barberi J., Verné E., Baino F., Bioactive glasses: from parent 45S5 composition to scaffold-assisted tissue-healing therapies, J. Funct. Biomater. 2018, 9, 24.
[6] Hench L.L., Genetic design of bioactive glass, J. Eur. Ceram. Soc. 2009, 29, 1257-1265.
[7] Hoppe A., Güldal N.S., Boccaccini A.R., A review of the biological response to ionic dissolution products from bioactive glasses and glass-ceramics, Biomaterials 2011, 32, 2757-2774.
[8] Kargozar S., Baino F., Hamzehlou S., Hill R.G., Mozafari M., Bioactive glasses entering the mainstream, Drug Discov. Today 2018, 23, 1700-1704.
[9] Hing K.A., Bioceramic bone graft substitutes: influence of porosity and chemistry, Int. J. Appl. Ceram. Technol. 2005, 2, 184-199.
[10] Karageorgiu V., Kaplan D., Porosity of 3D biomaterial scaffolds and osteogenesis, Biomaterials 2005, 26, 5474-5491.
[11] Miguez-Pacheco V., Hench L.L., Boccaccini A.R., Bioactive glasses beyond bone and teeth: Emerging applications in contact with soft tissues, Acta Biomater. 2015, 13, 1-15.
[12] Sanz-Herrera J.A., Garcia-Aznar J.M., Doblare M., A mathematical model for bone tissue regeneration inside a specific type of scaffold, Biomech. Model. Mechanobiol. 2008, 7, 355-366.
[13] Kohlhauser C. *et al.*, Ultrasonic characterisation of porous biomaterials across different frequencies, Strain 2009, 45, 34-44.
[14] Gerhardt L.C., Boccaccini A.R., Bioactive Glass and Glass-Ceramic Scaffolds for Bone Tissue Engineering, Materials 2010, 3, 2867-3910.
[15] Fu Q., Rahaman M.N., Bal B.S., Brown R.F., Day D.E., Mechanical and in vitro performance of 13–93 bioactive glass scaffolds prepared by a polymer foam replication technique, Acta Biomater. 4, 1854-1864 (2008).

[16] Baino F., Fiume E., Elastic mechanical properties of 45S5-based bioactive glass–ceramic scaffolds, Materials 2019, 12, 3244.
[17] Malasoma A. *et al.* Micromechanics of bioresorbable porous CEL2 glass ceramic scaffolds for bone tissue engineering, Adv. Appl. Ceram. 2008, 107, 277-286.
[18] Vitale-Brovarone C., Baino F., Bretcanu O., Verné E., Foam-like scaffolds for bone tissue engineering based on a novel couple of silicate-phosphate specular glasses: synthesis and properties, J. Mater. Sci. Mater. Med. 2009, 20, 2197-2205.
[19] Gibson L.J., Ashby F., The mechanics of three-dimensional cellular materials, Proc. R. Soc. Lond. A 1982, 382, 43-59.
[20] Falvo D'Urso Labate G., Catapano G., Vitale-Brovarone C., Baino F., Quantifying the micro-architectural similarity of bioceramic scaffolds to bone, Ceram. Int. 2017, 43, 9443-9450.
[21] Arnold M., Boccaccini A.R., Ondracek G., Prediction of the Poisson's ratio of porous materials, J. Mater. Sci. 1996, 31, 1643-1646.ù
[22] Warren W.E., Kraynik A.M., The linear elastic properties of open-cell foams, J. Appl. Mech. 1988, 55, 341-346.
[23] Zhu H.X., Knott J.F., Mills N.J., Analysis of the elastic properties of open-cell foams with tetrakaidecahedral cells, Mech. Phys. Solids 1997, 45, 319-343.
[24] Kraynik A.M., Warren W.E., The elastic behavior of low-density cellular plastics, In: N.C. Hilvard, A. Cunningham (Ed.), Low density cellular plastics, Chapman and Hall, London, 1994, pp. 187-225.
[25] Gan Y.X., Chen C., Shen Y.P., Three-dimensional modeling of the mechanical property of linearly elastic open cell foams, Int. J. Solids Struct. 2005, 42, 6628-6642.
[26] Roberts A.P., Garboczi E.J., Computation of the linear elastic properties of random porous materials with a wide variety of microstructure, Proc. R. Soc. Lond. A 2002, 458, 1033-1054.
[27] Nie Z., Lin Y., Ton Q., Computational modeling of the elastic property of three-dimensional open cell foams, Arch. Metall. Mater. 2018, 63, 1153-1165.
[28] Gibson L.J., Biomechanics of cellular solids, J. Biomech. 2005, 38, 377-399.
[29] De With G., Van Dijk H., Hattu N., Prijs K., Preparation, microstructure and mechanical properties of dense polycrystalline hydroxyapatite, J. Mater. Sci. 1981, 16, 1592-1598.
[30] Yu C., Ji S., Li Q., Effects of porosity on seismic velocities, elastic moduli and Poisson's ratios of solid materials and rocks, J. Rock Mech. Geotech. Eng. 2016, 8, 35-49.
[31] Torquato S., Effective stiffness tensor of composite media: II. Applications to isotropic dispersions, J. Mech. Phys. Solids 1998, 46, 1411–1440.
[32] Helte A., Fourth-order bounds on the effective bulk and shear moduli of random dispersions of penetrable spheres, Proc. R. Soc. Lond. A 1995, 450, 651–665.
[33] Lin C.Y., Kikuchia N., Hollister S.J., A novel method for biomaterial scaffold internal architecture design to match bone elastic properties with desired porosity, J. Biomech. 2004, 37, 623-636.
[34] Fritsch A., Dormieux L., Hellmich C., Sanahuja J., Mechanical behavior of hydroxyapatite biomaterials: an experimentally validated micromechanical model for elasticity and strength, J. Biomed. Mater. Res. A 2009, 88, 149-161.
[35] Scheiner S. *et al.*, Micromechanics of bone tissue-engineering scaffolds, based on resolution error-cleared computer tomography, Biomaterials 2009, 30, 2411-2419.
[36] Tagliabue S., Rossi E., Baino F., Vitale-Brovarone C., Gastaldi D., Vena P., Micro-CT based finite element models for elastic properties of glass–ceramic scaffolds, J. Mech. Behavior Biomed. Mater. 2017, 65, 248-255.
[37] Montazerian M., Zanotto E.D., Mauro J.C., Model-driven design of bioactive glasses: from molecular dynamics through machine learning, Int. Mater. Rev. 2020, 65, 297-321.
[38] Ravinder R. *et al.*, Predicting thermal, mechanical, and optical properties of oxide glasses by machine learning using large datasets, Mater. Horiz. 2020, 7, 1819-1827.